Preparation and Structural Characterization of Nitrosyl Complexes of Ferric Porphyrinates. Molecular Structure of Aquonitrosyl(*meso*-tetraphenylporphinato)iron(III) Perchlorate and Nitrosyl(octaethylporphinato)iron(III) Perchlorate

W. Robert Scheidt,*[1] Young Ja Lee,[1] and Keiichiro Hatano*[2]

Contribution from the Department of Chemistry, University of Notre Dame, Notre Dame, Indiana 46556, and the Department of Pharmaceutical Science, Nagoya City University, Nagoya, Japan 467. *Received November 10, 1983*

Abstract: Nitrosyl complexes of ferric porphyrinates have been prepared by reaction of (perchlorato)(porphyrinato)iron(III) complexes with nitric oxide. Two species have been structurally characterized: aquonitrosyl(*meso*-tetraphenylporphinato)iron(III) perchlorate, $[Fe(TPP)(NO)(H_2O)]ClO_4$, and nitrosyl(octaethylporphinato)iron(III) perchlorate, $[Fe(OEP)(NO)]ClO_4$. Crystal data for $[Fe(TPP)(NO)(H_2O)]ClO_4$: monoclinic, a = 10.303 (2) Å, b = 8.124 (2) Å, c = 21.364 (8) Å, and β = 97.76 (2)°, Z = 2, space group $P2_1/n$, 3999 observed data, R_1 = 0.057, R_2 = 0.079, with all measurements at 96 K. Crystal data for $[Fe(OEP)(NO)]ClO_4$; monoclinic, a = 12.890 (2) Å, b 20.363 (3) Å, c = 14.969 (2) Å, and β = 95.48 (2)°, Z = 4, space group $P2_1/n$, 5956 observed data, R_1 = 0.058, R_2 = 0.063, with all measurements at 292 K. All complexes are low-spin $\{FeNO\}^6$ species. $[Fe(OEP)(NO)]ClO_4$ is the first five-coordinate low-spin ferric porphyrinate to be structurally characterized. The Fe–N–O moiety is essentially linear in both species. For $[Fe(TPP)(NO)(H_2O)]ClO_4$, Fe–N_p = 1.999 (6) Å, Fe–N(NO) = 1.652 (5) Å, and Fe–O = 2.001 (5) Å. For $[Fe(OEP)(NO)]ClO_4$, Fe–N_p = 1.994 (1) Å and Fe–N(NO) = 1.644 (3) Å; the iron(III) atom is displaced 0.29 Å from the mean plane of the porphinato core. The structural parameters of both complexes are appropriate for low-spin ferric porphyrinates. $[Fe(OEP)(NO)]ClO_4$ forms a remarkable π–π dimer in the solid state. The two planar cores are parallel with an interplanar separation of only 3.36 Å.

The reactions of the diatomic molecules O_2, NO, CO, and CS with metalloporphyrins have been intensively investigated.[3] The interest in these reactions stems, of course, from their relevance to the biologically significant hemoproteins. Reactions of NO with hemes and hemoproteins are especially interesting. With the hemoproteins myoglobin and hemoglobin only one stable product is observed,[4] that corresponding to a $\{FeNO\}^7$ species,[5] irrespective of whether the protein was in the Fe(II) or Fe(III) form. Other hemoproteins, including horseradish peroxidase, cytochrome *c* peroxidase,[6] and cytochrome *c*,[7] react to yield stable ferric nitrosyl complexes. These are low-spin ferric derivatives and do not possess an EPR spectrum. The related ferrous species with peroxidases and cytochrome *c* can also be prepared; these derivatives are low-spin ($S = {}^1/_2$) compounds. In addition, nitrosyl complexes are possible intermediates in the catalytic cycle of assimilatory nitrite reductase, which catalyzes the six-electron reduction of nitrite to ammonia.[8,9] The prosthetic group of this enzyme is siroheme, an iron isobacteriochlorin complex. In the dissimilatory nitrite reductases, which catalyze the one-electron reduction of NO_2^- to NO, NO complexes of both oxidized and reduced hemes (formally Fe(III) and Fe(II)) have been detected.[10,11] Prosthetic groups in these enzymes are hemes *c* and *d*.

The reaction of NO with Fe(II) and Fe(III) porphyrinates yields five- and six-coordinate $\{FeNO\}^7$ species.[12-15] The ferric reactant is reduced via reductive nitrosylation in the presence of base, an apparently facile process.[12,13] However, Wayland and Olson[13] were able to demonstrate the existence of Fe(TPP)(Cl)(NO),[16] a formally ferric species, in toluene solution and Nujol mulls. More recently, Buchler et al.[17] reported that Fe(Porph)(NO) species can be reversibly oxidized to yield the $\{FeNO\}^6$ complexes $[Fe(Porph)(NO)]^+$. Olson et al.[18] have reported that oxidation of Fe(Porph)(NO) greatly increases the lability of the nitrosyl ligand, and attempts to isolate the oxidized species were unsuccessful. They further report that oxidation of Fe(Porph)(NO) under an atmosphere of NO allows the isolation of new ferric species, bis(nitrosyl) complexes, $[Fe(Porph)(NO)_2]ClO_4$.

We now wish to report the successful preparation and characterization of ferric mononitrosyl complexes. Aquonitrosyl(*meso*-tetraphenylporphinato)iron(III) perchlorate, $[Fe(TPP)(NO)(H_2O)]ClO_4$, and nitrosyl(octaethylporphinato)iron(III) perchlorate, $[Fe(OEP)(NO)]ClO_4$, are low-spin ferric complexes. The molecular structure of both compounds has been determined by X-ray diffraction techniques. Both have structural features appropriate for $\{FeNO\}^6$ complexes and are distinctly different

(1) University of Notre Dame.
(2) Nagoya City University.
(3) Recent reviews: Jameson, G. B.; Ibers, J. A. *Comments Inorg. Chem.* **1983**, *2*, 97-126. Collman, J. P. *Acc. Chem. Res.* **1977**, *10*, 265-272. Reed, C. A. In "Metal Ions in Biological Systems"; Sigel, H., Ed.; Marcel Dekker: New York, 1978, pp 277-310. Traylor, T. G. *Acc. Chem. Res.* **1981**, *14*, 102-109.
(4) Dickinson, L. C.; Chien, J. C. W. *J. Am. Chem. Soc.* **1971**, *93*, 5036-5140. Chien, J. C. W. *Ibid.* **1969**, *91*, 2166-2168.
(5) The notation is that of Enemark and Feltham (Enemark, J.; Feltham, R. *Coord. Chem. Rev.* **1974**, *13*, 339-406) and corresponds to a formal Fe(II) species.
(6) Yonetani, T.; Yamamoto, H.; Erman, J. E.; Leigh, J. S., Jr.; Reed, G. H. *J. Biol. Chem.* **1972**, *247*, 2447-2455.
(7) Ehrenberg, A.; Szczepkowski, T. W. *Acta Chem. Scand.* **1960**, *14*, 1684-1692.
(8) Vega, J. M.; Garrett, R. H.; Siegal, L. M. *J.* Biol. *Chem.* **1975**, *250*, 7980-7989.
(9) Vega, J. M.; Kamin, H. *Ibid.* **1977**, *252*, 896-909.
(10) Shimada, H.; Orii, Y. *FEBS Lett.* **1975**, *54*, 237-240.
(11) Johnson, M. K.; Thomson, A. J.; Walsh, T. A.; Barber, D.; Greenwood, C. *Biochem. J.* **1980**, *189*, 285-294.
(12) Scheidt, W. R.; Frisse, M. E. *J. Am. Chem. Soc.* **1975**, *97*, 17-21.
(13) Wayland, B. B.; Olson, L. W. *J. Am. Chem. Soc.* **1974**, *96*, 6037-6041.
(14) Scheidt, W. R.; Piciulo, P. *J. Am. Chem. Soc.* **1976**, *98*, 1913-1919.
(15) Scheidt, W. R.; Brinegar, A. C.; Ferro, E. B.; Kirner, J. F. *J. Am. Chem. Soc.* **1977**, *99*, 7315-7322.
(16) Abbreviations used: Porph, a generalized porphyrin dianion; TPP, the dianion of *meso*-tetraphenylporphyrin; OEP, the dianion of octaethylporphyrin; TTP, the dianion of *meso*-tetratolylporphyrin; TMP, the dianion of *meso*-tetramethylporphyrin; Ct, the center of the porphinato core; 1-MeIm, 1-methylimidaozle; 4-MePip, 4-methylpiperidine; das, *o*-phenylenebis(dimethylarsine); TMC, 1,4,8,11-tetramethyl-1,4,8,11-tetraazacyclotetradecane.
(17) Buchler, J. W.; Koskich, W.; Smith, P. D.; Tonn, B. *Z. Naturforsch., B: Anorg. Chem., Org. Chem.* **1978**, *338*, 1371-1380.
(18) Olson, L. W.; Schaeper, D.; Lancon, D.; Kadish, K. M. *J. Am. Chem. Soc.* **1982**, *104*, 2042-2044.

0002-7863/84/1506-3191$01.50/0

Table I. Summary of Crystal Data and Intensity Collection Parameters

	$[Fe(TPP)(NO)(H_2O)]ClO_4$	$[Fe(OEP)(NO)]ClO_4 \cdot CHCl_3$
formula	$FeClO_6N_5C_{44}H_{30}$	$FeCl_4O_5N_5C_{37}H_{45}$
fw, amu	816.1	837.5
space group	$P2_1/n$	$P2_1/n$
temp, K	96 ± 5	292 ± 1
a, Å	10.303 (2)	12.890 (2)
b, Å	8.124 (2)	20.363 (3)
c, Å	21.364 (8)	14.969 (2)
β, deg	97.76 (2)	95.48 (2)
V, Å^3	1772.0	3910.9
Z	2	4
d_{calcd}, g/cm^3	1.529	1.422
d_{obsd}, g/cm^3	1.48[a]	1.41
radiation	graphite—monochromated Mo Kα (λ = 0.71073 Å)	
scan technique	θ–2θ	θ–2θ
cryst dimens, mm	0.30 × 0.53 × 0.75	0.15 × 0.23 × 0.50
scan range	0.8° below Kα_1 0.8° above Kα_2	0.5° below Kα_1 0.5° above Kα_2
scan rate, deg/min	2–12	2–12
bckgrd	0.5 time scan time at the extremes of scan	
2θ limits, deg	3.5–56.80	3.5–54.90
criterion for observation	$F_o > 3\sigma(F_o)$	
unique obsd data	3999	5956
data/parameter	15.3	12.7
μ, mm^{-1}	0.56	0.71
R_1	0.057	0.058
R_2	0.079	0.063
goodness of fit	2.76	1.57

[a] Observed density at 292 K; calculated density from 292 K cell constants is 1.486 g/cm^3.

from those of porphinato $\{FeNO\}^7$ species previously characterized.[12,14,15] $[Fe(OEP)(NO)]ClO_4$ is the first low-spin ferric porphyrinato complex to be structurally characterized. This molecule also forms a remarkable π–π complex in the solid state, and features of this are described.

Experimental Section

Synthesis of $[Fe(TPP)(NO)(H_2O)]ClO_4$. $[Fe(TPP)(H_2O)_2]ClO_4$ was prepared from $[Fe(TPP)]_2O$ by reaction with 15% aqueous perchloric acid in $CHCl_3$ and crystallized by addition of *n*-pentane. $[Fe(TPP)(H_2O)_2]ClO_4$ (140 mg) was dissolved in 10 mL of hot $CHCl_3$ and the solution filtered. Benzene (4 mL) was added and the solution deoxygenated by bubbling purified N_2 through the solution. This solution was reacted with NO; the brown solution became red-brown. Single crystals were obtained by diffusing *n*-nonane into the reaction solution under an atmosphere of N_2/NO, yield 63 mg (40%). Attempts to recrystallize this isolated complex in the absence of NO were not successful, affording, inter alia, the starting aquo complex and $Fe(TPP)NO_3$[19] as judged from the IR spectrum. All infrared spectra were obtained as KBr pellets on a JASCO IRA-2 spectrometer. For $[Fe(TPP)(NO)(H_2O)]ClO_4$, the NO stretching frequency region has a peak at 1937 cm^{-1}. A broad band in the range of 1070–1115 cm^{-1} and a peak at 615 cm^{-1} are characteristic of the uncoordinated perchlorate ion. UV–vis absorption spectra were recorded on a Shimazu Model 200S spectrometer with use of a 1-cm quartz cell equipped with a stopcock connection to a vacuum line system. ESR spectra were recorded on a JEOL-FE3AX spectrometer at various temperatures from room temperature to 22 K. Single crystals (20 to 50 small pieces) were used as the sample without crushing or grinding. Magnetic susceptibilities were measured on a Faraday balance. μ = 1.72 μ_B at 298 K. Anal. Calcd for $[Fe(TPP)(NO)(H_2O)]ClO_4$, $FeClO_6N_5C_{44}H_{30}$: C, 64.77; H, 3.71; N, 8.59. Found: C, 63.55; H, 3.59; N, 8.09.

Synthesis of $[Fe(OEP)(NO)]ClO_4$. $Fe(OEP)OClO_3$ was prepared in a similar fashion as $[Fe(TPP)(H_2O)_2]ClO_4$. The red-brown solution of $Fe(OEP)OClO_3$ (50 mg) in 4 mL of $CHCl_3$ was reacted with NO under a N_2/NO atmosphere yielding a vivid pink solution. Single crystals were grown by allowing *n*-pentane to diffuse into the solution under an NO atmosphere. The infrared spectrum shows the NO stretching band at 1862 cm^{-1} and peaks at 1078, 1106, and 1147 cm^{-1} due to the perchlorate ion. A KBr pellet kept in a desiccator for a week does not show any significant changes in the IR spectrum, although the pink color of the product fades into a red-brown color almost immediately after dissolution in chloroform. Recrystallization attempts in air afforded mainly recovered $Fe(OEP)OClO_3$, μ = 1.06 μ_B at 298 K. Anal. Calcd for $[Fe(OEP)(NO)]ClO_4 \cdot CHCl_3$, $FeCl_4O_5N_5C_{37}H_{45}$: C, 53.07; H, 5.42; N, 8.37. Found: C, 53.03; H, 5.19; N, 8.39.

Structural Characterizations. Both crystalline species were subjected to preliminary examination on a Syntex P$\bar{1}$ diffractometer. Least-squares refinement of the setting angles of 60 reflections, collected at $\pm 2\theta$, gave the cell constants reported in Table I. All measurements utilized graphite-monochromated Mo Kα radation (λ 0.71073 Å). Data for $[Fe(TPP)(NO)(H_2O)]ClO_4$ were collected at 96 ± 5 K with use of an LT-1 low-temperature attachment for the diffractometer. Other details of the intensity collection parameters and refinements are summarized in Table I. Data were reduced as described previously.[20] Both structures were solved by the direct methods program MULTAN78.[21] Standard values for the atomic scattering factors including corrections for anomalous dispersion were employed in the structure analysis.

The two-molecule unit cell and the space group require that the $[Fe(TPP)(NO)(H_2O)]^+$ ion has a crystallographically imposed inversion center at the iron(III) atom. Thus, the two axial ligands must be disordered. Trial coordinates of the iron porphyrinate were established from MULTAN78. A difference Fourier synthesis established coordinates for the axial nitrosyl and aquo ligands. The perchlorate ion is disordered around the inversion center at $^1/_2$, 0, 0. The nitrosyl ligand and the prechlorate anion were treated as rigid groups in all subsequent cycles of least-squares refinement. For NO, an N–O bond length of 1.150 Å was used; the perchlorate ion was assigned T_d symmetry with Cl–O = 1.420 Å. Both species were assigned occupancy factors of 0.5 as required by the symmetry of the problem. After a few cycles of full-matrix least-squares refinement, a difference Fourier showed a second orientation of the perchlorate group. This group was remodeled as two rigid groups, with each atom of the group assigned an atomic occupancy of 0.25. Additional refinement, followed by difference Fourier syntheses, led to the location of all hydrogen atoms of the porphinato ligand. The hydrogen

(19) Phillippi, M. A.; Baenziger, N.; Goff, H. M. *Inorg. Chem.* **1981**, *20*, 3904–3911.

(20) Scheidt, W. R. *J. Am. Chem. Soc.* **1974**, *96*, 84–89.

(21) Programs used in this study included local modifications of Main, Hull, Lessinger, Germain, Declerq, and Woolfson's MULTAN78, Jacobson's ALFF and ALLS, Busing and Levy's ORFFE and ORFLS, and Johnson's ORTEP2. Atomic form factors were from Cromer and Mann: Cromer, D. T.; Mann, J. B. *Acta Crystallogr., Sect. A* **1968**, *A24*, 321–323. Real and imaginary corrections for anomalous dispersion in the form factor of the iron and chlorine atoms were from Cromer and Liberman: Cromer, D. T.; Liberman, D. J. *J. Chem. Phys.* **1970**, *53*, 1891–1898. Scattering factors for hydrogen were from Stewart et al.: Stewart, R. F.; Davidson, E. R.; Simpson, W. T. *Ibid.* **1965**, *42*, 3175–3187.

Table II. Fractional Coordinates for Aquonitrosyl(*meso*-tetraphenylporphinato)iron(III) Perchlorate[a]

atom	*x*	*y*	*z*
Fe	0.0	0.0	0.0
N(1)	−0.09667 (18)	0.18752 (22)	0.03250 (8)
N(2)	−0.04644 (18)	0.08473 (21)	−0.08823 (8)
O(1)	−0.1644 (4)	−0.1340 (6)	−0.00830 (21)
C(a1)	−0.11367 (21)	0.21815 (25)	0.09456 (10)
C(a2)	−0.16015 (21)	0.31472 (25)	−0.00194 (10)
C(a3)	−0.12138 (20)	0.22096 (25)	−0.10707 (9)
C(a4)	−0.00982 (23)	0.01807 (25)	−0.14252 (10)
C(b1)	−0.18398 (22)	0.36911 (26)	0.09896 (10)
C(b2)	−0.21210 (23)	0.42882 (26)	0.03981 (10)
C(b3)	−0.13501 (22)	0.23587 (27)	−0.17463 (10)
C(b4)	−0.06593 (23)	0.11246 (27)	−0.19627 (10)
C(m1)	−0.06646 (22)	0.12228 (26)	0.14661 (9)
C(m2)	−0.17508 (20)	0.33088 (25)	−0.06744 (9)
C(1)	−0.10228 (23)	0.17219 (26)	0.20977 (10)
C(2)	−0.01064 (24)	0.24326 (28)	0.25584 (10)
C(3)	−0.04671 (28)	0.28617 (29)	0.31439 (11)
C(4)	−0.1723 (3)	0.2576 (3)	0.32698 (11)
C(5)	−0.26429 (27)	0.1897 (3)	0.28091 (12)
C(6)	−0.22913 (25)	0.14786 (28)	0.22220 (11)
C(7)	−0.25330 (20)	0.47419 (25)	−0.09611 (9)
C(8)	−0.38561 (23)	0.48937 (27)	−0.08931 (12)
C(9)	−0.45688 (22)	0.6252 (3)	−0.11456 (13)
C(10)	−0.39817 (23)	0.7459 (3)	−0.14595 (11)
C(11)	−0.26781 (23)	0.73213 (28)	−0.15344 (10)
C(12)	−0.19540 (20)	0.59595 (26)	−0.12864 (9)

[a] The estimated standard deviations of the least significant digits are given in parentheses.

Table III. Group Parameters for Aquonitrosyl(*meso*-tetraphenylporphinato)iron(III) Perchlorate[a]

param	value	param	value	param	value
		Group N–O			
x	0.1331 (5)	φ	2.098 (7)	B_{group}	0.0
y	0.1152 (8)	θ	3.139 (8)	B_1	1.94 (12)
z	0.0048 (3)	ρ	0.3449	B_2	3.14 (6)
		Group ClO_4			
x	0.5030 (3)	θ	2.446 (6)	B_2	8.7 (5)
y	0.0470 (5)	ρ	−0.302 (9)	B_3	11.1 (5)
z	−0.00715 (18)	B_{group}	0.0	B_4	2.66 (11)
φ	0.587 (10)	B_1	3.71 (9)	B_5	5.92 (28)
		Group ClO_4'			
x	0.48875 (25)	θ	2.528 (3)	B_2	1.72 (13)
y	0.0553 (3)	ρ	−0.969 (6)	B_3	4.43 (18)
z	0.00137 (13)	B_{group}	0.0	B_4	4.45 (17)
φ	0.766 (4)	B_1	2.33 (6)	B_5	1.80 (9)

Derived Crystallographic Coordinates for the Group Atoms

group	atom	*x*	*y*	*z*
N–O	N(3)	0.1331	0.1152	0.0048
	O(2)	0.2296	0.1864	0.0049
ClO_4	Cl(1)	0.5030	0.0470	−0.0072
	O(3)	0.4460	0.2063	−0.0139
	O(4)	0.4044	−0.0738	−0.0230
	O(5)	0.6001	0.0318	−0.0480
	O(6)	0.5613	0.0238	0.0563
ClO_4'	Cl(2)	0.4888	0.0553	0.0014
	O(7)	0.4504	0.2207	−0.0122
	O(8)	0.3819	−0.0333	0.0204
	O(9)	0.5271	−0.0188	−0.0535
	O(10)	0.5957	0.0525	0.0508

[a] The estimated standard deviations of the least significant digits are given in parentheses.

atoms were idealized (C–H = 0.95 Å, B(H) = B(C) + 1.0 Å^2) and included in all subsequent refinement cycles as fixed contributors with additional reidealization as required. Refinement was then carried to convergence with anisotropic temperature factors for all heavy atoms except those of the rigid groups. At convergence, the final values for the discrepancy indices were R_1 = 0.057 and R_2 = 0.079.[22] The final data/variable ratio as 15.3. A final difference Fourier map was judged to be essentially featureless; the largest peak was 0.7 e/Å^3 and was located near the iron atom. A table of final atomic coordinates is given in Table II. The rigid group parameters and derived crystallographic coordinates for the nitrosyl ligand and the perchlorate anion are given in Table III. Table IV details the anisotropic temperature factors of the atoms and is given in the supplementary material. A final listing of observed and calculated structure amplitudes (×10) is also available as supplementary material.

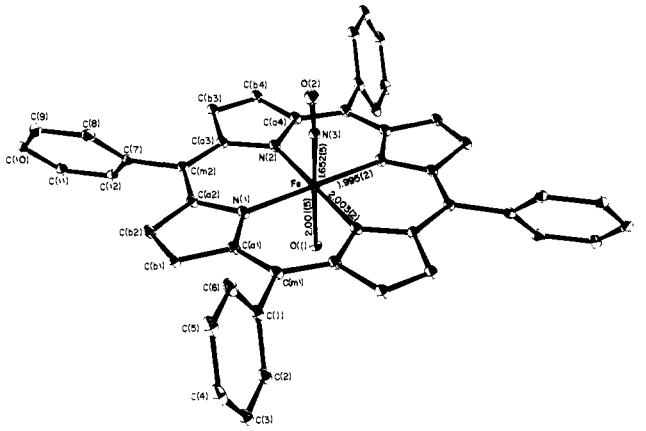

Figure 1. Computer-drawn model, in perspective, of the [Fe(TPP)(NO)(H_2O)]ClO_4 molecule. The labeling scheme used for the molecule is shown. Also displayed are the bond distances in the coordination group of the molecule. Ellipsoids in all drawings are contoured at the 50% probability level.

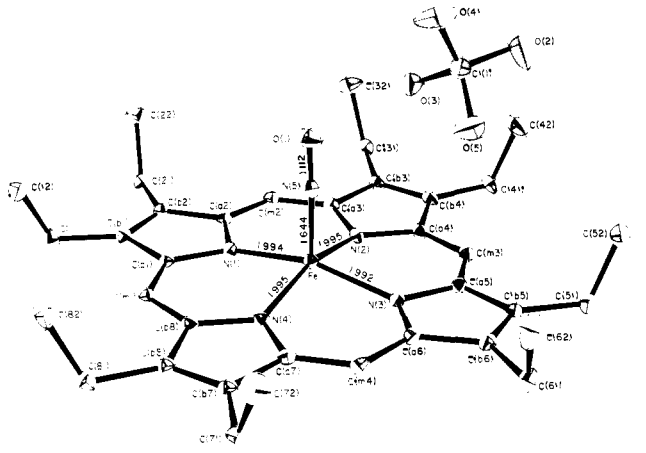

Figure 2. Computer-drawn model of the [Fe(OEP)(NO)]ClO_4 molecule. The figure also displays the bond distances in the coordination group and the labeling scheme used for the atoms.

The structure solution and refinement of [Fe(OEP)(NO)]ClO_4 was routine. Difference Fourier calculations revealed the positions of the meso hydrogen atoms and most of the positions of the hydrogen atoms of the ethyl groups. All hydrogen atoms were included in subsequent cycles of least-squares refinement as idealized fixed contributors. At convergence, R_1 = 0.058 and R_2 = 0.063; the final data/variable ratio was 12.7. The final difference Fourier synthesis was free of any significant features. The values for the final atomic coordinates are given in Table V. Final anisotropic temperature factors (Table VI) and calculated and observed structure amplitudes (×10) are available as supplementary material.

Results and Discussion

We first consider the structural results. Figures 1 and 2 present the molecular structures of [Fe(TPP)(NO)(H_2O)]ClO_4 and [Fe(OEP)(NO)]ClO_4, respectively. Both figures illustrate the labeling scheme for the unique atoms of the molecles and the bond distances in the coordination group. Data collection for [Fe(T-

(22) $R_1 = \sum||F_o| - |F_c||/\sum|F_o|$ and $R_2 = [\sum w(|F_o| - |F_c|)^2/\sum w(F_o)^2]^{1/2}$.

Table V. Fractional Coordinates for Nitrosyl(octaethylporphinato)iron(III) Perchlorate[a]

atom	x	y	z
Fe	0.35315 (3)	0.452448 (22)	−0.00835 (3)
Cl(1)	0.30036 (11)	0.24643 (7)	0.82429 (8)
Cl(2)	0.31657 (11)	0.25417 (7)	0.14506 (10)
Cl(3)	0.14691 (12)	0.17095 (10)	0.08072 (12)
Cl(4)	0.35715 (13)	0.12190 (8)	0.09511 (12)
N(1)	0.38252 (19)	0.45074 (12)	0.12483 (17)
N(2)	0.48509 (19)	0.40251 (12)	−0.01658 (17)
N(3)	0.35537 (20)	0.47675 (13)	−0.13703 (17)
N(4)	0.25534 (19)	0.52705 (12)	0.00448 (17)
N(5)	0.26887 (23)	0.39170 (15)	−0.01931 (19)
O(1)	0.20963 (23)	0.35187 (15)	−0.02382 (22)
O(2)	0.3467 (4)	0.2066 (4)	0.7650 (3)
O(3)	0.36484 (29)	0.25331 (20)	0.90583 (22)
O(4)	0.2079 (3)	0.21876 (23)	0.8418 (4)
O(5)	0.2875 (5)	0.30807 (27)	0.7870 (3)
C(a1)	0.32401 (25)	0.47908 (16)	0.18721 (21)
C(a2)	0.45095 (25)	0.41005 (15)	0.17529 (21)
C(a3)	0.53830 (24)	0.36592 (15)	0.05073 (22)
C(a4)	0.52538 (24)	0.38203 (16)	−0.09408 (23)
C(a5)	0.41205 (25)	0.44651 (16)	−0.19973 (21)
C(a6)	0.28355 (25)	0.51530 (17)	−0.18812 (22)
C(a7)	0.19810 (25)	0.56150 (15)	−0.06297 (22)
C(a8)	0.21262 (24)	0.54659 (16)	0.08160 (22)
C(b1)	0.35695 (25)	0.45651 (16)	0.27677 (21)
C(b2)	0.43605 (26)	0.41413 (16)	0.26951 (22)
C(b3)	0.61342 (26)	0.32228 (16)	0.01483 (24)
C(b4)	0.60574 (25)	0.33281 (16)	−0.07462 (23)
C(b5)	0.37600 (27)	0.46689 (17)	−0.28912 (22)
C(b6)	0.29579 (27)	0.50893 (17)	−0.28268 (22)
C(b7)	0.12238 (25)	0.60350 (16)	−0.02720 (23)
C(b8)	0.13055 (25)	0.59424 (16)	0.06256 (22)
C(m1)	0.24563 (25)	0.52409 (16)	0.16616 (22)
C(m2)	0.52399 (25)	0.37115 (16)	0.14019 (22)
C(m3)	0.49168 (25)	0.40331 (16)	−0.17850 (22)
C(m4)	0.21231 (26)	0.55613 (16)	−0.15277 (23)
C(11)	0.30809 (29)	0.47708 (19)	0.35968 (23)
C(12)	0.2070 (4)	0.44270 (26)	0.3718 (3)
C(21)	0.49869 (28)	0.37710 (17)	0.34311 (23)
C(22)	0.4578 (4)	0.30865 (20)	0.35776 (28)
C(31)	0.67753 (28)	0.27323 (19)	0.06942 (26)
C(32)	0.6135 (4)	0.21292 (22)	0.0904 (3)
C(41)	0.66422 (28)	0.29901 (19)	−0.14392 (26)
C(42)	0.6091 (4)	0.23924 (24)	−0.1833 (4)
C(51)	0.42050 (28)	0.44260 (19)	−0.37252 (23)
C(52)	0.3762 (4)	0.37787 (22)	−0.40627 (28)
C(61)	0.2278 (3)	0.54202 (20)	−0.35717 (24)
C(62)	0.1223 (4)	0.50926 (28)	−0.3756 (3)
C(71)	0.04592 (29)	0.64663 (19)	−0.08289 (25)
C(72)	−0.0436 (3)	0.60872 (24)	−0.1293 (3)
C(81)	0.06740 (29)	0.62445 (18)	0.13048 (25)
C(82)	−0.0146 (3)	0.57960 (24)	0.1630 (3)
C(1)	0.2778 (4)	0.19112 (24)	0.0700 (3)

[a] The estimated standard deviations of the least significant digits are given in parentheses.

PP)(NO)(H_2O)]ClO_4 was carried out at 96 K to retard decomposition of the complex. The concomitant dampening of the thermal motion also aided in the resolution of the disordered coordination group of [Fe(TPP)(NO)(H_2O)]ClO_4. The success of the disorder refinement is suggested by the closely similar values for the Fe–N(NO) bond distances is the two complexes.

Individual values for bond distances and bond angles for [Fe(TPP)(NO)(H_2O)]ClO_4 are given in Tables VII and VIII. Corresponding values for [Fe(OEP)(NO)]ClO_4 are given in Tables IX and X. Averaged values for the bond parameters in the core of [Fe(TPP)(NO)(H_2O)]ClO_4 are displayed in Figure 3. Averaged values for [Fe(OEP)(NO)]ClO_4 are shown in Figure 4. The values in parentheses are the estimated standard deviations calculated by using the population of individual averaged values.

Table VII. Bond Lengths in [Fe(TPP)(NO)(H_2O)]$^+$ [a]

type	length, Å	type	length, Å
Fe–N(1)	1.995 (2)	C(a4)–C(m1)′	1.394 (3)
Fe–N(2)	2.003 (2)	C(b1)–C(b2)	1.348 (3)
Fe–N(3)	1.652 (5)	C(b3)–C(b4)	1.347 (3)
Fe–O(1)	2.001 (5)	C(1)–C(m1)	1.502 (3)
N(1)–C(a1)	1.383 (3)	C(1)–C(2)	1.394 (3)
N(1)–C(a2)	1.381 (3)	C(1)–C(6)	1.383 (3)
N(2)–C(a3)	1.378 (3)	C(2)–C(3)	1.396 (3)
N(2)–C(a4)	1.378 (3)	C(3)–C(4)	1.377 (4)
N(3)–O(2)[b]	1.150	C(4)–C(5)	1.386 (4)
C(a1)–C(b1)	1.434 (3)	C(7)–C(m2)	1.499 (3)
C(a1)–C(m1)	1.391 (3)	C(7)–C(8)	1.396 (3)
C(a2)–C(b2)	1.439 (3)	C(7)–C(12)	1.389 (3)
C(a2)–C(m2)	1.393 (3)	C(8)–C(9)	1.393 (4)
C(a3)–C(b3)	1.436 (3)	C(9)–C(10)	1.374 (4)
C(a3)–C(m2)	1.395 (3)	C(10)–C(11)	1.379 (3)
C(a4)–C(b4)	1.436 (3)		

[a] The numbers in parentheses are the estimated standard deviations. Primed and unprimed symbols denote a pair of atoms related by the inversion center at Fe. [b] Bond length assigned for group refinement.

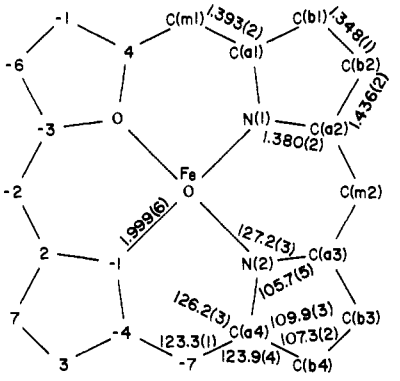

Figure 3. Formal diagram of the porphinato core in [Fe(TPP)(NO)(H_2O)]ClO_4. The perpendicular displacement of each unique atom, in units of 0.01 Å, from the mean plane of the prophinato core is displayed. Also shown in the figure are the averaged bond distances and angles of the unique chemical classes in the core.

The two figures also display perpendicular displacements, in units of 0.01 Å, of each atom from the mean plane of the 24-atom core. In neither structure is the deviation from planarity remarkable.

The bonding parameters of the two coordination groups are those expected[23] for low-spin iron(III) porphyrinates. The average Fe–N_p bond distances of 1.999 (6) Å in [Fe(TPP)(NO)(H_2O)]ClO_4 and 1.994 (1) Å in [Fe(OEP)(NO)]ClO_4 are both marginally longer than the 1.990-Å average value for six-coordinate low-spin iron(III) porphyrinate derivatives,[23] but they are within the range observed. The out-of-plane displacement of the iron(III) atom in low-spin six-coordinate porphyrinates is typically quite small (0.0 to <0.09 Å). This is also the case for [Fe(TPP)(NO)(H_2O)]ClO_4. Although the crystallographic disorder does not permit an exact determination of the displacement, the reasonableness of the temperature factors of the iron(III) atom and the axial bond distances (calculated assuming no displacement) clearly suggest a small (<0.05 Å) displacement of the iron(III) atom. For five-coordinate [Fe(OEP)(NO)]ClO_4, a displacement of the iron(III) atom toward the axial ligand can be expected. The observed displacements are 0.32 Å from the N_4 plane and 0.29 Å from the mean plane of the 24-atom core. Although there are no other structurally characterized low-spin five-coordinate (porphinato)iron(III) complexes available for comparison, these

(23) Scheidt, W. R.; Reed, C. A. *Chem. Rev.* **1981**, *81*, 543–555.

Table VIII. Bond Angles in $[Fe(TPP)(NO)(H_2O)]^+$ [a]

angles	value, deg	angles	value, deg	angles	value, deg	angles	value, deg
N(1)FeN(2)	89.89 (7)	C(b2)C(a2)C(m2)	124.20 (20)	FeN(2)C(a3)	127.16 (13)	C(a3)C(b3)C(b4)	107.32 (19)
N(1)FeN(3)	89.71 (23)	N(2)C(a3)C(b3)	109.64 (17)	FeN(2)C(a4)	126.81 (14)	C(a4)C(b4)C(b3)	107.29 (18)
N(1)FeO(1)	89.41 (14)	N(2)C(a3)C(m2)	126.11 (19)	C(a3)N(2)C(a4)	106.03 (17)	C(a1)C(m1)C(a4)′	123.17 (19)
N(2)FeN(3)	87.41 (25)	C(b3)C(a3)C(m2)	124.25 (20)	FeN(3)O(2)	174.4 (10)	C(a1)C(m1)C(1)	117.73 (19)
N(2)FeO(1)	90.67 (14)	N(2)C(a4)C(b4)	109.68 (18)	N(1)C(a1)C(b1)	110.31 (18)	C(a4)′C(m1)C(1)	119.08 (19)
N(3)FeO(1)	177.89 (26)	N(2)C(a4)C(m1)′	126.51 (20)	N(1)C(a1)C(m1)	126.15 (19)	C(a2)C(m2)C(a3)	123.37 (20)
FeN(1)C(a1)	127.20 (14)	C(b4)C(a4)C(m1)′	123.78 (19)	C(b1)C(a1)C(m1)	123.50 (18)	C(a2)C(m2)C(7)	117.65 (18)
FeN(1)C(a2)	127.49 (13)	C(a1)C(b1)C(b2)	107.03 (18)	N(1)C(a2)C(b2)	109.93 (18)	C(a3)C(m2)C(7)	118.98 (18)
C(a1)N(1)C(a2)	105.31 (16)	C(a2)C(b2)C(b1)	107.36 (19)	N(1)C(a2)C(m2)	125.86 (18)		

[a] The numbers in parentheses are the estimated standard deviations. Primed and unprimed symbols denote a pair of atoms related by the inversion center of Fe.

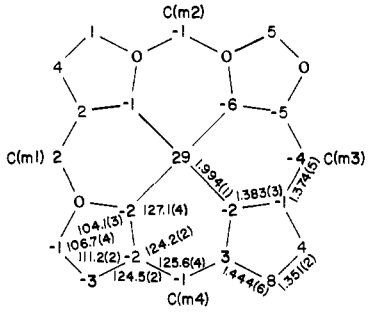

Figure 4. Formal diagram of the porphinato core in $[Fe(OEP)(NO)]ClO_4$ displaying the same information as Figure 3. Positive values of the displacements are toward the axial NO ligand. The Ct···N radius in the molecule is 1.973 Å.

displacements can be compared with those observed in a series of $M^{II}(TPP)(NO)$ complexes (M = Mn,[24] Fe[12], and Co[25]). In this series, the Ct··· M displacement follows the order Mn (0.34 Å) > Fe (0.21 Å) > Co (0.09 Å). The M–N(NO) bond distances in the series also vary (inversely) with values 1.641, 1.717, and 1.833 Å, respectively. However, in the series there are essentially constant N(NO)···N(Porph) nonbonded contacts of 2.76 to 2.79 Å, and the C···N(NO) distances vary over the narrow range of 1.93 to 1.98 Å. It was suggested[24] that the metal atom displacements result from the effect of nonbonded repulsions between the NO nitrogen atom and atoms of the porphinato core; the metal atom displacements vary to maintain a minimum N(NO)···N(Porph) separation of ~2.8 Å. The values observed in $[Fe(OEP)(NO)]ClO_4$ also fit this pattern: Ct···N(NO) = 1.964 Å and N(NO)···N(Porph) = 2.781 Å. We conclude that the relatively large Fe(III) out-of-plane displacement (compared to other low-spin iron porphyrinates) is predominantly determined by nonbonded repulsions.

A comparison of the axial bonding parameters of $[Fe(TPP)(NO)(H_2O)]ClO_4$ and $[Fe(OEP)(NO)]ClO_4$ with several $\{FeNO\}^7$ metalloporphyrin complexes and with the isoelecronic $\{MnNO\}^6$ species, [Mn(TTP)NO] and [Mn(TPP)(NO)(4-MePip)], is given in Table XI. The $\{FeNO\}^6$ complexes are expected to have shorter Fe–N(NO) bonds and a more nearly linear Fe–N–O group relative to the $\{FeNO\}^7$ species. As can be seen from Table XI, this is indeed observed. The length of the Fe–N(NO) bonds is comparable to those of the $\{MnNO\}^6$ species and also to other $\{FeNO\}^6$ complexes: 1.621 (6) Å in $[Fe(TMC)(NO)(OH)](BF_4)_2$,[26] 1.63 (2) Å in $Na_2[Fe(CN)_5(NO)]$,[27] and 1.62–1.67 Å for a number of other nitroprusside salts.[28] Consistent with the low-spin state of $[Fe(TPP)(NO)(H_2O)]ClO_4$, the axial Fe–O bond is significantly shorter than the 2.095 (2)-Å value found for high-spin $[Fe(TPP)(H_2O)_2]ClO_4$.[29] The $\{FeNO\}^7$ complexes listed in Table XI all display a significant lengthening of the bond trans to the NO ligand; this is not expected nor observed in the $\{FeNO\}^6$ complex.

The cations of $[Fe(TPP)(NO)(H_2O)]ClO_4$ are well separated in the crystalline lattice. In contrast, there is an unexpected and interesting set of intermolecular interactions for $[Fe(OEP)(NO)]ClO_4$. In its lattice, the cations interact in pairs to form π–π dimers. A stereoview of the unit cell contents is shown in Figure 5. Although π–π dimer interactions in metalloporphyrin

Table IX. Bond Lengths in $[Fe(OEP)(NO)]ClO_4 \cdot CHCl_3$ [a]

bond type	length, Å	bond type	length, Å
Fe–N(1)	1.994 (3)	C(a8)–C(m1)	1.375 (4)
Fe–N(2)	1.995 (3)	C(b1)–C(b2)	1.348 (4)
Fe–N(3)	1.992 (3)	C(b1)–C(11)	1.504 (5)
Fe–N(4)	1.995 (3)	C(b2)–C(21)	1.505 (4)
Fe–N(5)	1.644 (3)	C(b3)–C(b4)	1.350 (5)
N(1)–C(a1)	1.381 (4)	C(b3)–C(31)	1.490 (5)
N(1)–C(a2)	1.381 (4)	C(b4)–C(41)	1.506 (5)
N(2)–C(a3)	1.382 (4)	C(b5)–C(b6)	1.353 (5)
N(2)–C(a4)	1.380 (4)	C(b5)–C(51)	1.506 (5)
N(3)–C(a5)	1.387 (4)	C(b6)–C(61)	1.509 (5)
N(3)–C(a6)	1.387 (4)	C(b7)–C(b8)	1.351 (4)
N(4)–C(a7)	1.383 (4)	C(b7)–C(71)	1.510 (5)
N(4)–C(a8)	1.384 (4)	C(b8)–C(81)	1.494 (5)
N(5)–O(1)	1.112 (4)	C(11)–C(12)	1.505 (6)
C(a1)–C(b1)	1.442 (4)	C(21)–C(22)	1.514 (5)
C(a1)–C(m1)	1.378 (4)	C(31)–C(32)	1.529 (6)
C(a2)–C(b2)	1.444 (4)	C(41)–C(42)	1.502 (6)
C(a2)–C(m2)	1.373 (4)	C(51)–C(52)	1.504 (5)
C(a3)–C(b3)	1.454 (4)	C(61)–C(62)	1.517 (6)
C(a3)–C(m2)	1.373 (4)	C(71)–C(72)	1.503 (6)
C(a4)–C(b4)	1.451 (4)	C(81)–C(82)	1.512 (6)
C(a4)–C(m3)	1.367 (4)	Cl(1)–O(2)	1.380 (5)
C(a5)–C(b5)	1.435 (4)	Cl(1)–O(3)	1.416 (3)
C(a5)–C(m3)	1.366 (4)	Cl(1)–O(4)	1.366 (4)
C(a6)–C(b6)	1.445 (4)	Cl(1)–O(5)	1.377 (5)
C(a6)–C(m4)	1.381 (5)	C(1)–Cl(2)	1.747 (5)
C(a7)–C(b7)	1.439 (4)	C(1)–Cl(3)	1.759 (5)
C(a7)–C(m4)	1.378 (5)	C(1)–Cl(4)	1.761 (5)
C(a8)–C(b8)	1.444 (4)		

[a] The numbers in parentheses are the estimated standard deviations.

(24) Scheidt, W. R.; Hatano, K.; Rupprecht, G. A.; Piciulo, P. L. *Inorg. Chem.* **1979**, *18*, 292–299.
(25) Scheidt, W. R.; Hoard, J. L. *J. Am. Chem. Soc.* **1973**, *95*, 8281–8288.
(26) Hodges, K. D.; Wollmann, R. G.; Kessel, S. L.; Hendrickson, D. N.; Van Derveer, D. G.; Barefield, E. K. *J. Am. Chem. Soc.* **1979**, *101*, 906–917.
(27) Manoharan, P. T.; Hamilton, W. C. *Inorg. Chem.* **1963**, *2*, 1043–1047.
(28) Punte, G.; Rigotti, G.; Irvero, B. E.; Podjarny, A. D. *Acta Crystallogr., Sect. B* **1980**, *B36*, 1472–1475. Rigotti, G.; Punte, G.; Rivero, B. E.; Castellano, E. E. *Ibid.* **1980**, *B36*, 1475–1477. Castellano, E. E.; Piro, O. E.; Rivero, B. E. *Ibid.* **1977**, *B33*, 1725–1728 and 1728–1732.
(29) Scheidt, W. R.; Cohen, I. A.; Kastner, M. E. *Biochemistry* **1979**, *18*, 3546–3552.

Table X Bond Angles in $[Fe(OEP)(NO)]ClO_4 \cdot CHCl_3$

type	angles, deg	type	angles, deg	type	angles, deg	type	angles, deg
N(1)FeN(2)	88.35 (10)	C(b8)C(a8)C(m1)	124.2 (3)	N(1)C(a1)C(b1)	111.34 (27)	C(a8)C(b8)C(81)	125.4 (3)
N(1)FeN(3)	162.28 (11)	C(a1)C(b1)C(b2)	106.67 (28)	N(1)C(a1)C(m1)	123.98 (29)	C(b7)C(b8)C(81)	128.6 (3)
N(1)FeN(4)	88.76 (10)	C(a1)C(b1)C(11)	124.68 (29)	C(b1)C(a1)C(m1)	124.7 (3)	C(a1)C(m1)C(a8)	126.00 (27)
N(1)FeN(5)	98.47 (12)	C(b2)C(b1)C(11)	128.6 (3)	N(1)C(a2)C(b2)	111.22 (28)	C(a2)C(m2)C(a3)	125.4 (3)
N(2)FeN(3)	88.62 (11)	C(a2)C(b2)C(b1)	106.73 (28)	N(1)C(a2)C(m2)	124.2 (3)	C(a4)C(m3)C(a5)	125.8 (3)
N(2)FeN(4)	160.76 (10)	C(a2)C(b2)C(21)	125.0 (3)	C(b2)C(a2)C(m2)	124.5 (3)	C(a6)C(m4)C(a7)	125.2 (3)
N(2)FeN(5)	99.75 (12)	C(b1)C(b2)C(21)	128.2 (3)	N(2)C(a3)C(b3)	111.20 (28)	C(b1)C(11)C(12)	113.9 (3)
N(3)FeN(4)	88.37 (10)	C(a3)C(b3)C(b4)	106.32 (29)	N(2)C(a3)C(m2)	124.46 (28)	C(b2)C(21)C(22)	113.4 (3)
N(3)FeN(5)	99.25 (12)	C(a3)C(b3)C(31)	124.1 (3)	C(b3)C(a3)C(m2)	124.3 (3)	C(b3)C(31)C(32)	111.6 (3)
N(4)FeN(5)	99.49 (12)	C(b4)C(b3)C(31)	129.4 (3)	N(2)C(a4)C(b4)	111.03 (29)	C(b4)C(41)C(42)	113.0 (3)
FeN(1)C(a1)	127.22 (21)	C(a4)C(b4)C(b3)	106.98 (29)	N(2)C(a4)C(m3)	124.7 (3)	C(b5)C(51)C(52)	113.8 (3)
FeN(1)C(a2)	127.42 (21)	C(a4)C(b4)C(41)	124.9 (3)	C(b4)C(a4)C(m3)	124.2 (3)	C(b6)C(61)C(62)	112.6 (3)
C(a1)N(1)C(a2)	104.02 (25)	C(b3)C(b4)C(41)	128.1 (3)	N(3)C(a5)C(b5)	110.97 (28)	C(b7)C(71)C(72)	112.8 (3)
FeN(2)C(a3)	126.61 (21)	C(a5)C(b5)C(b6)	107.35 (29)	N(3)C(a5)C(m3)	124.1 (3)	C(b8)C(81)C(82)	114.4 (3)
FeN(2)C(a4)	126.68 (21)	C(a5)C(b5)C(51)	124.2 (3)	C(b5)C(a5)C(m3)	124.9 (3)	O(2)Cl(1)O(3)	110.9 (3)
C(a3)N(2)C(a4)	104.46 (25)	C(b6)C(b5)C(51)	128.4 (3)	N(3)C(a6)C(b6)	111.09 (29)	O(2)Cl(1)O(4)	108.6 (3)
FeN(3)C(a5)	126.95 (22)	C(a6)C(b6)C(b5)	106.4 (3)	N(3)C(a6)C(m4)	124.3 (3)	O(2)Cl(1)O(5)	108.5 (4)
FeN(3)C(a6)	127.12 (22)	C(a6)C(b6)C(61)	125.0 (3)	C(b6)C(a6)C(m4)	124.6 (3)	O(3)Cl(1)O(4)	109.08 (27)
C(a5)N(3)C(a6)	104.19 (26)	C(b5)C(b6)C(61)	128.6 (3)	N(4)C(a7)C(b7)	111.30 (28)	O(3)Cl(1)O(5)	107.28 (27)
FeN(4)C(a7)	127.86 (21)	C(a7)C(b7)C(b8)	107.21 (29)	N(4)C(a7)C(m4)	124.08 (29)	O(4)Cl(1)O(5)	112.4 (4)
FeN(4)C(a8)	127.20 (21)	C(a7)C(b7)C(71)	124.8 (3)	C(b7)C(a7)C(m4)	124.6 (3)	Cl(2)C(1)Cl(3)	109.3 (3)
C(a7)N(4)C(a8)	103.65 (25)	C(b8)C(b7)C(71)	127.9 (3)	N(4)C(a8)C(b8)	111.77 (27)	Cl(2)C(1)Cl(4)	109.04 (25)
FeN(5)O(1)	176.9 (3)	C(a8)C(b8)C(b7)	106.04 (29)	N(4)C(a8)C(m1)	124.00 (29)	Cl(3)C(1)Cl(4)	109.65 (25)

[a] The numbers in parentheses are the estimated standard deviations.

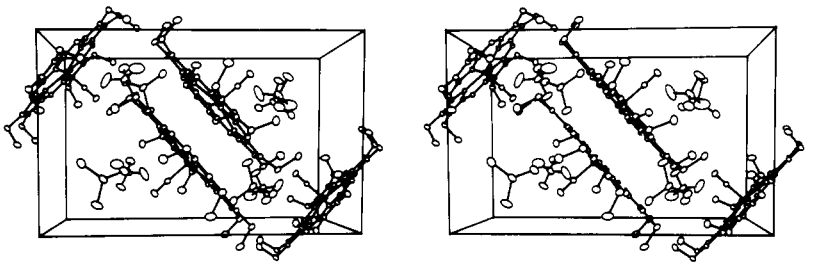

Figure 5. A stereoscopic view of the packing for $[Fe(OEP)(NO)]ClO_4$. The origin is at the lower left corner of the cell nearest the viewer. The horizontal axis is the *b* axis and is positive moving left to right. The vertical axis is the *a* axis and is positive moving up the page. The *c* axis is in the direction away from the viewer.

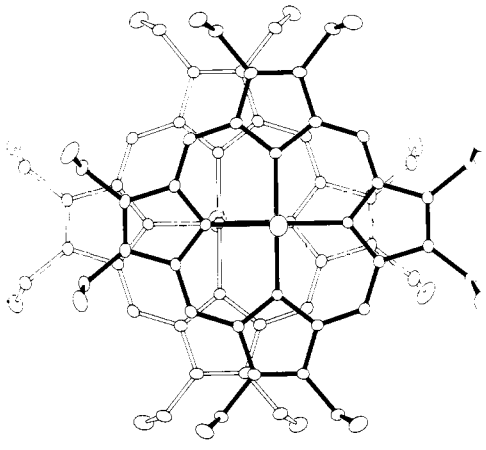

Figure 6. A computer-drawn model of the two $[Fe(OEP)(NO)]^+$ ions related by an inversion center showing the overlap of the two cores. The planes of the two parallel porphinato cores are parallel to the plane of the paper, and the heavy-lined core is closest to the viewer.

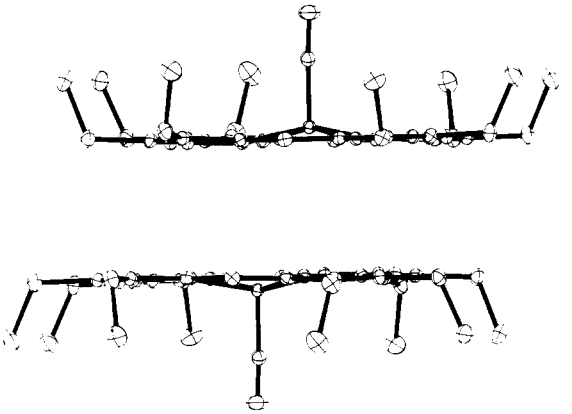

Figure 7. A second view of the π–π dimer in the lattice of $[Fe(OEP)(NO)]ClO_4$. The two porphinato cores are perpendicular to the plane of the drawing.

species have been recognized for some time,[30] the feature in $[Fe(OEP)(NO)]ClO_4$ that commands interest is the tightness of the interaction. The stereochemical nature of the π–π interaction can be seen in Figures 6 and 7. The two $[Fe(OEP)(NO)]^+$ ions in Figures 6 and 7 are related by an inversion center; consequently, the two porphinato planes are precisely parallel. Figure 6 is a veiw perpendicular to the porphinato planes that clearly shows the "slipped" nature of the π–π complex. Figure 7 is a view parallel to the two porphinato planes. The mean separation

(30) Blumberg, W. E.; Peisach, J. *J. Biol. Chem.* **1965**, *240*, 870–876.

Table XI. Comparison of Axial Bonding Parameters in {MNO}^{6} and {MNO}^{7} Metalloporphyrins[a]

metalloporphyrin	distances, Å				angles, deg	ref
	M–Np	M–N(NO)	M–Ct[b]	M–Ax[c]	M–N–O	
[Fe(OEP)(NO)]ClO_4	1.994 (1)	1.644 (3)	0.32		176.9 (3)	this work
[Fe(TPP)(NO)(H_2O)]ClO_4	1.999 (6)	1.652 (5)	~0	2.001 (5)	174.4 (10)	this work
[Mn(TTP)(NO)]	2.004 (5)	1.641 (2)	0.34		177.8 (3)	24
[Mn(TPP)(NO)(4-MePip)]	2.027 (3)	1.644 (5)	0.10	2.206 (5)	176.2 (5)	24
[Fe(TPP)(NO)(1-MeIm)]	2.008 (12)	1.743 (4)	0.07	2.180 (4)	142.1 (6)	14
[Fe(TPP)(NO)(4-MePip)]·$CHCl_3$ solvate	2.004 (10)	1.721 (10)	0.09	2.328 (10)	138.5 (11)	15
[Fe(TPP)(NO)(4-MePip)]	1.999 (10)	1.740 (7)	0.11	2.463 (7)	143.7 (6)	15
[Fe(TPP)(NO)]	2.001 (3)	1.717 (7)	0.21		149.2 (6)	12

[a] Numbers in parentheses are the estimated standard deviations. [b] All metal atom displacements are toward the NO ligand. [c] Ax is the axial ligand donor atom.

Table XII. Nonbonded Intermolecular Contacts between Porphinato Cores Less than 3.6 Å

type	distance, Å	type	distance, Å
N(1)···C(m3)[a]	3.444	C(a1)···C(m3)[a]	3.385
N(1)···C(a5)[a]	3.476	C(a2)···C(a5)[a]	3.415
N(3)···C(m2)[a]	3.468	C(a6)···C(m2)[a]	3.417
N(3)···C(a2)[a]	3.485	C(a7)···C(b3)[a]	3.419
N(4)···C(b4)[a]	3.478	C(a8)···C(b4)[a]	3.402
N(4)···C(b3)[a]	3.529	C(b2)···C(b5)[a]	3.419
N(4)···C(a4)[a]	3.534	C(b8)···C(41)[a]	3.548
N(4)···C(a3)[a]	3.596		

[a] Atoms are related to the reported atomic coordinates by ($1 - x$, $1 - y$, $-z$).

between the two planes is a very tight 3.362 Å, well within the 3.2–3.5-Å separation generally recognized[31] to indicate π–π interaction. The perpendicular distance between the two N_4 planes is slightly smaller, 3.287 Å. The Fe···Fe′ separation is 4.238 Å and the Ct to Ct′ separation is 3.652 Å. The observed arrangement can be formally derived from two completely eclipsed porphinato cores which are then laterally shifted with respect to each other by 1.43 Å in the direction of an Fe–N_p bond. A detailed listing of the interatomic contacts less than 3.6 Å is given in Table XII. A similar dimer has been observed for crystals of Fe(OEP)-$OClO_3$,[32] but this species has a larger interplane distance (3.53 Å), a larger lateral shift (3.39 Å), and a Ct···Ct′ separation of 4.89 Å. A similar interplanar spacing has been observed in Ni(TMP).[33] However, the porphyrin cores show much larger lateral shifts (Ct···Ct′ = 5.66 Å) and concomitant smaller overlap between pairs of porphinato cores. Other π complexes that involve a porphyrin and a second aromatic molecule include toluene–porphyrin[34] and tetracyanoquinodimethane–porphyrin[35] complexes.

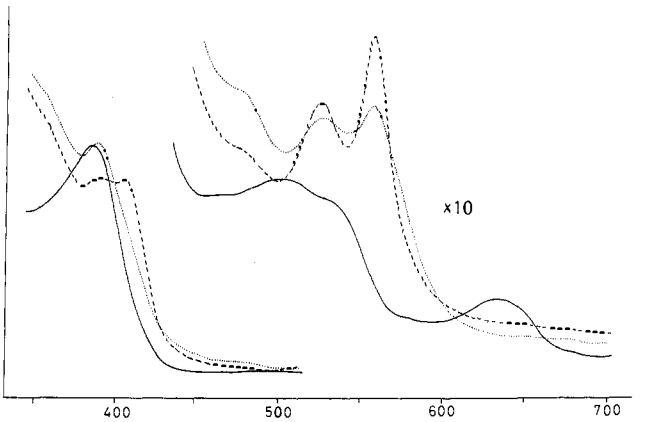

Figure 8. Spectral changes during the reaction of Fe(OEP)$OClO_3$ with NO in $CHCl_3$ at 18 ± 2 °C: (—) 4.9×10^{-6} M Fe(OEP)$OClO_3$; (- - -) 94 torr of NO added; and (···) 211 torr of NO.

Similar (3.30 to 3.37 Å) interplanar spacings are observed.

Structural information for dimeric porphyrin species in solution has been obtained by NMR[36] and EPR[30,37] techniques. The structural models derived from these studies are qualitatively similar to that observed for [Fe(OEP)(NO)]ClO_4 in the solid state; however, the lateral shifts and interplanar spacings derived from the solution measurements are generally larger.

The observed NO stretching frequencies (1862 cm^{-1} for [Fe(OEP)(NO)]ClO_4 and 1937 cm^{-1} for [Fe(TPP)(NO)(H_2O)]ClO_4) are well outside the range of 1625 to 1675 cm^{-1} observed[15] for the analogous iron(II) species. The increase in stretching frequency is expected.[5] Similar stretching frequencies are seen for other {FeNO}^{6} complexes: $Na_2[Fe(CN)_5(NO)]$[38] (1939 cm^{-1}), $[Fe(das)_2(NO)(NCS)]^{2+}$[39] (1885 cm^{-1}), and [Fe(TMC)(NO)-(OH)]$(BF_4)_2$[26] (1890 cm^{-1}).

The structural results and other physical data clearly confirm the synthesis of nitrosyl iron(III) porphyrinates. However, it is also clear that the ferric nitrosyl complexes have only limited stability and readily convert to other species. As noted in the Experimental Section, the complexes cannot be successfully crystallized in the absence of an NO atmosphere. However, too great an excess of NO can lead to reductive nitrosylation. In dilute ($\sim 5 \times 10^{-6}$ M) chloroform solution, the reaction of NO with [Fe(TPP)(H_2O)$_2$]ClO_4 is not reversible upon evacuation; the solution spectrum is ultimately that of Fe(TPP)NO.[12] The reaction of Fe(OEP)$OClO_3$ with NO is at least partially reversible. Reactions under increased NO pressure lead to decreasing reversibility. However, comparison of spectra (Figure 8) at all pressures of NO with spectra of $[Fe(OEP)(NO)]^+$ produced

(31) Herbstein, F. H. *Perspect. Struct. Chem.* **1971**, *4*, 166–395.
(32) Masuda, H.; Taga, T.; Osaki, K.; Sugimoto, H.; Yoshida, Z.-I.; Ogoshi, H. *Inorg. Chem.* **1980**, *19*, 950–955.
(33) Kutzler, F. W.; Swepston, P. N.; Berkovitch-Yellin, Z.; Ellis, D. E.; Ibers, J. A. *J. Am. Chem. Soc.* **1983**, *105*, 2996–3004.
(34) Kirner, J. F.; Reed, C. A.; Scheidt, W. R. *J. Am. Chem. Soc.* **1977**, *99*, 1093–1101. Scheidt, W. R.; Kastner, M. E.; Hatano, K. *Inorg. Chem.* **1978**, *17*, 706–710. Scheidt, W. R.; Reed, C. A. *Ibid.* **1978** *17*, 710–714.
(35) Pace, L. J.; Ulman, A.; Ibers, J. A. *Inorg. Chem.* **1982**, *21*, 199–207.
(36) Abraham, R. J.; Burbidge, P. A.; Jackson, A. H.; Macdonald, D. B. *J. Chem. Soc. B* **1966**, 620–626. Abraham, R. J.; Evans, B.; Smith, K. M. *Tetrahedron* **1978**, *34*, 1213–1219. Snyder, R. V.; LaMar, G. N. *J. Am. Chem. Soc.* **1977**, *99*, 7178–7184.
(37) Chikira, M.; Kon, H.; Hawley, R. A.; Smith, K. M. *J. Chem. Soc., Dalton Trans.* **1979**, 245–249. MacCragh, A.; Storm, C. B.; Koski, W. S. *J. Am. Chem. Soc.* **1965**, *87*, 1470–1476. Boas, J. F.; Pilbrow, J. R.; Smith, T. D. *J. Chem. Soc. A* **1969**, 721–723. Boyd, P. D. W.; Smith, T. D.; Price, J. H.; Pilbrow, J. R. *J. Chem. Phys.* **1972**, *56*, 1253–1263.
(38) Paliani, G.; Poletti, A.; Santucci, A. *J. Mol. Struct.* **1971**, *8*, 63–74.
(39) Nappier, T. E.; Feltham, R. D.; Enemark, J. H.; Kruse, A.; Cooke, M. *Inorg. Chem.* **1975**, *14*, 806–815.

electrochemically[40,41] suggests that the reaction system always contain nitrosyl species other than $[Fe(OEP)(NO)]^+$. The higher than expected magnetic moments are the evident result of small amounts of iron(III) impurities[42] and a low-spin iron(II) impurity. EPR spectra confirm the presence of low levels of a high-spin iron(III) contaminant ($g = 6$) and small amounts of a low-spin species as well.[43] $[Fe(TPP)(NO)(H_2O)]ClO_4$ is more susceptible to this decomposition,[44] and as noted previously, X-ray data collection was carried out at 96 K to retard this decomposition.

Acknowledgment. The support of this work by the National Institutes of Health (Grant HL-15627) is gratefully acknowledged. We thank Prof. Mitsuo Sato (Teikyo University) for EPR spectra.

Registry No. $[Fe(TPP)(NO)(H_2O)]ClO_4$, 89596-91-8; $[Fe(OEP)(NO)]ClO_4$, 89596-93-0.

Supplementary Material Available: Table IV, anisotropic temperature factors for $[Fe(TPP)(NO)(H_2O)]ClO_4$, Table VI, anisotropic temperature factors for $[Fe(OEP)(NO)]ClO_4$, and listings of observed and calculated structure amplitudes for both complexes (37 pages). Ordering information is given on any current masthead page.

(40) Fujita, E.; Fajer, J. *J. Am. Chem. Soc.* **1983**, *105*, 6743-6745.
(41) Lancon, D.; Kadish, K. M. *J. Am. Chem. Soc.* **1983**, *105*, 5610-5617.
(42) The moments correspond to impurity levels of between 3 and 8% of a high-spin iron(III) species of comparable molecular weight. The level of these high-spin impurities increases with time. Magnetic moments were measured at least 2 weeks after prepration owing to the necessity of sending samples from Nagoya to Notre Dame.
(43) This is possibly a nitrosyl iron(II) species. EPR parameters for this species contained in crystals of $[Fe(OEP)(NO)]ClO_4$ are $g_\perp = 2.052$, $g_\parallel = 2.010$, $A_{N\parallel} = 17.7$ G, and $A_{N\perp} = 19.1$ G.
(44) This is in accord with recently reported electrochemical results reported in ref 41.

Origin of the High Ligand Field Strength and Macrocyclic Enthalpy in Complexes of Nitrogen-Donor Macrocycles

Vivienne J. Thöm, Jan C. A. Boeyens, Gloria J. McDougall, and Robert D. Hancock*

Contribution from the Department of Chemistry, University of the Witwatersrand, Johannesburg, South Africa. *Received February 14, 1983*

Abstract: The relationship between hole size in the cavities of tetraaza macrocycles, the strain-free M-N bond lengths for various metal ions, and the occurrence of the maximum value of the in-plane ligand field (LF) strength, $Dq_{(xy)}$, as a function of the size of the macrocyclic cavity, is discussed. It is shown that the maximum value of $Dq_{(xy)}$ occurs when the metal ion fits best into the cavity, rather than when the metal ion is compressed (Busch, 1971) by the macrocycle. It is shown by using empirical force-field calculations (EFF) that Co(III) is too small for an exact fit into most polyamine ligand systems, with a strain-free Co-N length of 1.925 Å. Nonbonded repulsions between adjacent ligands at such short M-N lengths prevent such short bond lengths being realized for virtually all complexes of Co(III) with polyamines, except for unusual circumstances, as found in complexes with macrocycles, such as 13-aneN_4 (1,4,7,11-tetraazacyclotridecane). The effect of steric strain on LF strength is investigated, and a simple model is developed which relates strain in the M-N bond to the LF strength. This model supports the idea that the high LF strength in complexes of macrocyclic ligands is due to a large number of secondary nitrogen donors in a situation of comparatively low strain in the M-N bond. EFF calculations are then used to calculate enthalpies of complex formation of complexes of polyamines with Ni(II) in aqueous solution, assuming that solvation effects can be neglected, and it is suggested on the basis of these calculations that the macrocyclic enthalpy is due to (1) the inductive effects of the extra secondary nitrogens in the macrocycle and (2) the high state of steric strain in the macrocyclic ligand, brought about by dipole-dipole repulsion in the gas phase, and a contribution from steric hindrance to solvation in aqueous solution.

The extra stability of the complexes of macrocyclic ligands over that of their open-chain analogues has been termed the macrocyclic effect.[1] The extra thermodynamic stability is usually, but not always, in the nitrogen-donor macrocycles, accompanied by a stronger ligand field.[2,3] It is generally agreed that the entropy contribution to the macrocyclic effect is due to the smaller configurational entropy of the macrocycle as compared with the open-chain ligand. Our interest in this paper is the origin of the enthalpy contribution, and, perhaps even more interesting, the stronger ligand field, in complexes of N-donor macrocycles.

Busch et al.[2-4] have suggested that the above stronger ligand field is produced by compression of the metal ion by the encircling macrocycle. They have carried out empirical force-field (EFF) calculations on the free macrocyclic ligands and determined the M-N bond lengths of coordinated metal ions which produce the least strain in the resulting complex. These best-fit metal-nitrogen bond lengths are shown in Table I. Busch et al. have further noted[3] that the ligand field strength of a metal ion such as Co(III) in a series of analogous complexes with the series of macrocycles 13-aneN_4 through 16-aneN_4 varies with the ring size of the macrocycle such that the ligand field (LF) is at a maximum for a particular ring size. Thus, for Co(III) this occurs in 13-aneN_4,

(1) Cabbiness, D. K.; Margerum, D. W. *J. Am. Chem. Soc.* **1969**, *91*, 6540-6541.
(2) Busch, D. H.; Farmery, K.; Goedken, V.; Katovic, V.; Melnyk, A. C.; Sperati, C. R.; Tokel, N. *Adv. Chem. Ser.* **1971**, *No. 100*, 44-78.
(3) Hung, Y.; Martin, L. Y.; Jackels, S. C.; Tait, A. M.; Busch, D. H. *J. Am. Chem. Soc.* **1977**, *99*, 4029-4039.
(4) Busch, D. H. *Acc. Chem. Res.* **1978**, *11*, 392-400.

0002-7863/84/1506-3198$01.50/0